

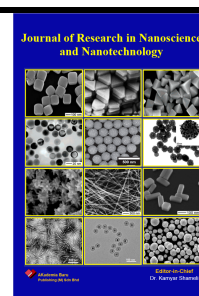


## Journal of Research in Nanoscience and Nanotechnology

Journal homepage:

<http://akademiabaru.com/submit/index.php/jrnn/index>

ISSN: 2773-6180



# Effect of Cerium Oxides Loaded Nitric Acid-Treated Palm Kernel Shell Biochar on Pyrolysis of High-Density Polyethylene

Tang Kui Ee<sup>1</sup>, Vekes Balasundram<sup>1,\*</sup>, Norazana Ibrahim<sup>2</sup>, Ruzinah Isha<sup>3</sup>, Le Kim Pham Hoang<sup>4</sup>, Suan Shi<sup>5,\*</sup>

<sup>1</sup> Malaysia-Japan International Institute of Technology (MJIIT), Universiti Teknologi Malaysia, Jalan Sultan Yahya Petra, 54100 Kuala Lumpur, Malaysia

<sup>2</sup> Faculty of Chemical and Energy Engineering, Universiti Teknologi Malaysia, 81310 Johor Bahru, Johor, Malaysia

<sup>3</sup> Faculty of Chemical and Process Engineering Technology, Universiti Malaysia Pahang Al-Sultan Abdullah, Lebuhr Persiaran Tun Khalil Yaakob, 26300 Kuantan, Pahang, Malaysia

<sup>4</sup> Faculty of Applied Science and Technology, Nguyen Tat Thanh University, Ho Chi Minh City 755414, Viet Nam

<sup>5</sup> Engineering Laboratory for Agro Biomass Recycling & Valorizing, College of Engineering, China Agricultural University, Beijing 100083, China

\* Correspondence: vekes@utm.my

<https://doi.org/10.37934/jrnn.16.1.6070>

## ABSTRACT

This study aims to evaluate the physicochemical properties of cerium oxides loaded nitric acid-treated palm kernel shell biochar (Ce/NA-PKSBC) and examine their catalytic performance in the pyrolysis of high-density polyethylene (HDPE). The catalyst was prepared in two steps, first via pyrolysis and then the incipient wetness impregnation method, and characterised for surface morphology and textural properties. Pyrolysis was conducted at 500°C in a fixed-bed horizontal reactor, with oil product analysis performed using gas chromatography/ mass spectrometry (GC/MS). For comparison, the non-catalytic, raw PKSBC, and NA-PKSBC catalysts were also pyrolysed under the same conditions. The results indicate that the Ce/NA-PKSBC exhibited improved surface morphology and significantly enhanced textural properties compared to PKSBC, and Ce/NA-PKSBC has the highest surface area at 369.62 m<sup>2</sup>/g compared to other synthesized catalysts. For pyrolysis results, the non-catalytic achieved the highest pyrolysis oil + wax at 91% followed by NA-PKSBC (68%), PKSBC (60%), and Ce/NA-PKSBC (46%). Ce/NA-PKSBC achieved notable yields of hydrocarbons at 93.25%. These findings suggest that Ce-modified represent a viable and sustainable alternative to

\* Corresponding author.

E-mail address: vekes@utm.my (Vekes Balasundram)

<https://doi.org/10.37934/jrnn.16.1.6070>

conventional catalysts, offering high efficiency and environmental compatibility for converting plastic waste into fuel.

*Keywords:*

Plastic waste; Pyrolysis; Biochar; Cerium  
Oxides; Fuel; Hydrocarbons

Received: 15 July 2025

Revised: 30 July 2025

Accepted: 21 August 2025

Published: 25 August 2025

## 1. Introduction

The recent global energy crisis has underscored the fragility of the energy sector in the face of disruptions, such as the COVID-19 pandemic [1]. These challenges have not only disrupted supply chains but have also led to significant fluctuations in energy prices, further emphasizing the intricate interconnections within global markets. As fossil fuels continue to dominate as the primary energy source, their limited availability and detrimental environmental impact have intensified the call for the development of alternative, sustainable energy solutions [2]. Concurrently, the issue of plastic waste generation has escalated dramatically. In Southeast Asia, Malaysia stands out as one of the largest producers and importers of plastics, grappling with significant challenges in managing this mounting waste stream [3]. The prevalence of single-use plastics and packaging is particularly concerning, as plastics account for approximately 22% of the daily municipal solid waste in the country [4]. Ineffective disposal practices, such as open dumping and uncontrolled incineration, not only contribute to greenhouse gas emissions but also exacerbate environmental pollution.

Moreover, traditional waste management practices like landfilling and incineration prove to be unsustainable solutions. They release toxic gases and leave behind persistent residues that harm ecosystems and human health [5]. To address these intertwined crises of energy and plastic waste, there is an urgent need for innovative approaches that focus on sustainability, which could include transitioning to renewable energy sources and adopting circular economy principles in plastic production and consumption. Only through comprehensive strategies can we mitigate the environmental impact while enhancing resilience in both energy and waste management systems.

Pyrolysis offers a promising pathway for addressing both energy and waste management challenges by converting plastics into valuable hydrocarbon products [5]. Its performance, however, is strongly dependent on the use of effective catalysts, which influence reaction rates, cracking efficiency, and product selectivity. Conventional catalysts such as zeolites (HZSM-5, USY, and beta zeolite) have demonstrated high activity but are prone to deactivation from coke deposition, reducing operational stability [6]. Metal oxides and transition metals have been incorporated into catalyst systems to mitigate these issues, but many remain costly, toxic, or environmentally burdensome. Moreover, many synthetic catalysts are costly, non-renewable, and require energy-intensive manufacturing, raising environmental concerns [7].

Biochar-based catalysts represent a renewable, cost-effective, and environmentally friendly alternative. Produced via biomass pyrolysis, biochar features high surface area, tuneable porosity, abundant oxygen-containing functional groups, and a thermally stable carbon structure [8]. These properties enhance the dispersion of active metals, improve catalyst-reactant interactions, and provide additional active sites for cracking. Importantly, pre-treatment of biochar with nitric acid has been shown to further improve its performance as a catalyst support by introducing additional carboxyl, hydroxyl, and nitro functional groups [9]. These functionalities enhance surface acidity,

increase wettability, and act as anchoring sites for metal ions, thereby improving the uniformity and stability of metal dispersion during impregnation [9]. Despite these advantages, the application of nitric acid-treated biochar in the catalytic pyrolysis of plastics remains limited, making it an underexplored yet promising research direction. Among potential metal modifications, cerium oxide ( $\text{CeO}_2$ ) offers unique catalytic benefits due to its high oxygen storage capacity, redox flexibility ( $\text{Ce}^{3+}/\text{Ce}^{4+}$  cycling), and strong resistance to coke formation [10]. These characteristics enable prolonged catalytic activity, promote selective C–C bond cleavage, and improve hydrocarbon product distribution. When loaded onto nitric acid-treated PKS biochar, cerium's benefits can be amplified by enhanced dispersion, better active site accessibility, and increased thermal stability of the support.

This study investigates the effect of cerium oxides loaded onto nitric acid-treated palm kernel shell biochar (Ce/NA-PKSBC) on the pyrolysis of high-density polyethylene (HDPE). PKSBC was selected for its abundance as an agricultural residue in Malaysia, renewable nature, and favourable physicochemical properties. The catalytic performance of Ce/NA-PKSBC was evaluated in terms of product yields and hydrocarbon selectivity, aiming to address both the drawbacks of conventional catalysts and the lack of systematic studies on functionalised biochar-supported cerium oxides for plastic waste conversion.

## 2. Methodology

### 2.1 Catalyst Preparation

The palm kernel shell was collected from a local palm mill in Selangor, Malaysia. The production of palm kernel shell biochar (PKSBC) was carried out through pyrolysis in a horizontal fixed-bed reactor, as depicted in Figure 1. The experimental setup included a fixed-bed reactor, a tubular furnace for heating, a condenser system, a gas collection bag, and a nitrogen supply to maintain an inert atmosphere. Before the experiment, 20 g of palm kernel shell powder was loaded into crucible boats. All input and output connections were tightly secured to prevent leakage. Nitrogen gas was used to purge the reactor with a flow rate of 80 mL/min. The pressure was maintained at atmospheric pressure (1 atm).

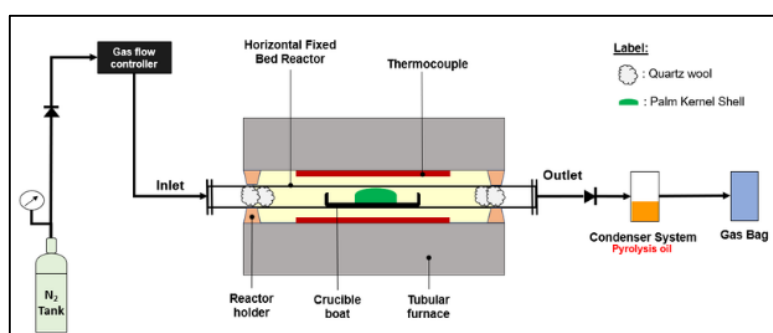


**Fig. 1.** Schematic diagram of pyrolysis of biochar setup

The tubular furnace was heated to the target reaction temperature of  $800^\circ\text{C}$  using an electronic control panel for an hour to produce the PKSBC. The pyrolysis oil condensed in the condenser system was disposed of, microparticles and soluble gases were captured in a gas bag. After each experiment and once the reactor had cooled down, the reactor was disassembled, and biochar was recovered. The

produced biochar was collected and sieved to 50 microns using a planetary ball mill. Finally, it was labelled PKSBC and stored in a desiccator to prevent moisture absorption.

Next, to produce nitric acid-treated PKSBC, the PKSBC was soaked in a 10% nitric acid solution, stirred with a magnetic stirrer at 80°C for 4 hours. The treated PKSBC was rinsed with deionised water at 80°C, and then the biochar was separated from the acid solution using a vacuum filter. The process was repeated until a pH of approximately seven was detected with a pH meter. Finally, the nitric acid-treated PKSBC was labelled as NA-PKSBC.

Next, the incipient wetness impregnation (IWI) method was used to develop cerium oxide-modified catalyst. First, cerium (III) nitrate hexahydrate ( $\text{Ce}(\text{NO}_3)_3 \cdot 6\text{H}_2\text{O}$ , 99% purity) was purchased from ACROS Organics. Next, 1 wt.% cerium salts and 99 wt.%, and 80 mL deionized water were mixed in a beaker. Then, the mixture was transferred to a hot plate magnetic stirrer and stirred thoroughly for 4 hours at 80°C. Afterwards, the mixture was dried in a microwave oven at 105°C until the weight remained constant, to remove moisture. Finally, the dried solid was transferred into a tube furnace for calcination at 600°C for 3 hours under a nitrogen atmosphere to thermally stabilise the catalyst. The resulting catalyst was collected, sieved to 50 microns, and labelled as Ce/NA-PKSBC. All the synthesized catalysts were characterized for their physicochemical properties such as phase analysis, surface morphology, and textural properties (surface area, total pore volume, and average pore diameter). The detailed steps of characterization techniques can be found in our previous work [10].

## 2.2 Catalytic Pyrolysis

The effects of Ce/NA-PKSBC catalyst on the pyrolysis of HDPE were evaluated using a laboratory-scale fixed-bed reactor, as shown in Figure 2. The experimental setup included a fixed-bed reactor, a tubular furnace for heating, a condenser system, a gas collection bag, and a nitrogen ( $\text{N}_2$ ) supply to maintain an inert atmosphere. HDPE as pyrolysis feedstock was collected from a local waste management company in Klang, Malaysia. The obtained feedstock was in pellet form with a size of 5 mm and kept in a sealed container to avoid contamination. Before the experiment, 2g of the synthesized catalyst and 6g of HDPE pellets were kept separate in two different crucible boats to facilitate catalyst recovery; then both were placed into the fixed-bed reactor, maintaining a catalyst-to-plastic ratio of 1:3 by mass. All input and output connections were securely tightened to prevent leakage.  $\text{N}_2$  was used to purge the reactor, ensuring an inert and non-reactive environment, with a flow rate of 80 mL/min. The experiments were conducted under atmospheric pressure (1 atm).

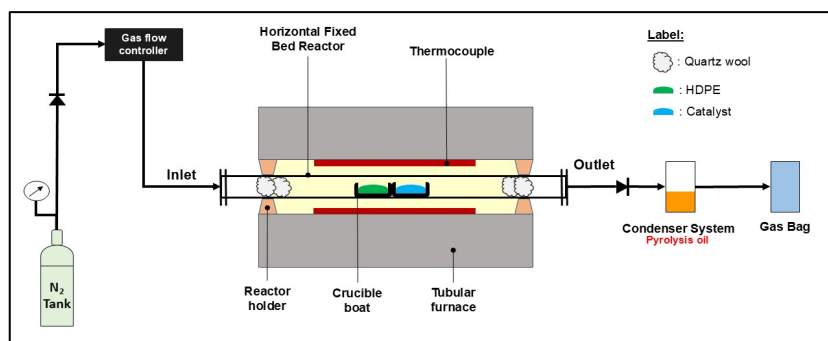


Fig. 2. Schematic diagram pyrolysis setup

In the experiment, the temperature remained constant as the tubular furnace was heated to the target reaction temperature of 500°C. The pyrolysis process was carried out for one hour, including cooling time. As the pyrolysis reaction proceeded, the resulting volatile compounds were carried by the nitrogen stream out of the reactor and directed into a condenser system, where a filtering flask immersed in room temperature water (maintained at 25°C) condensed the vapours. The gaseous products were condensed into pyrolysis oil, which was collected and analysed to determine its chemical composition via gas chromatography/mass spectrometry (GC/MS, Agilent, G3171A) to identify hydrocarbon yield. The standard operating procedures for GC/MS analysis were reported in our previous work [10]. Meanwhile, microparticles and non-condensable gases were captured in a gas bag. After each experiment, the reactor was disassembled and cooled to room temperature, and the residual solid materials were recovered and weighed.

### 3. Result and Discussion

#### 3.1. Surface Morphology

The surface morphology of all synthesized catalysts at a magnification of  $\times 10,000$  is shown in Figure 3. As observed in Figure 3 (a), PKSBC exhibits a porous, irregular surface structure with limited visible microstructural pores. This suggests that PKSBC has a lower surface area and reduced surface reactivity. In detail, the formation and diameter of pores appear inconsistent. These pores are essential for exposing active sites and facilitating mass transfer during catalytic reactions.

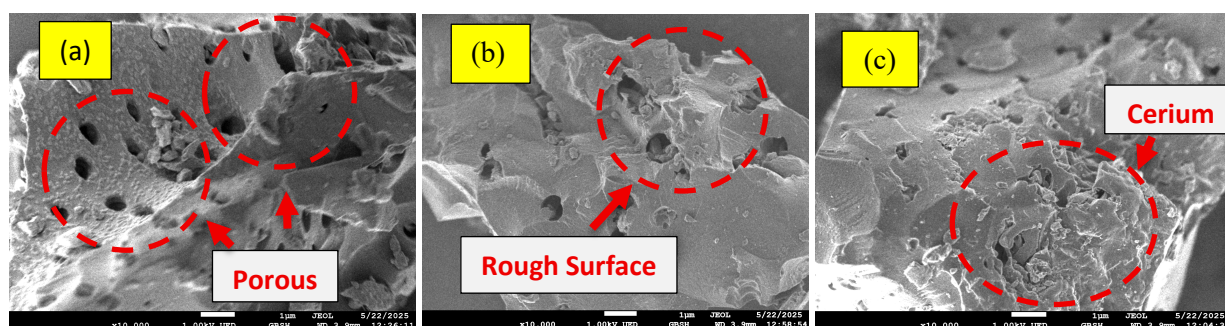


Fig. 3. Surface morphology of (a) PKSBC, (b) NA-PKSBC, and (c) Ce/NA-PKSBC

The surface morphology of PKSBC aligns with the findings of Dechapanya and Khamwichit (2023) [8], who also developed biochar from palm kernel shells for biosorption. Meanwhile, the surface morphology of NA-PKSBC demonstrates a noticeable increase in surface roughness and porosity, as shown in Figure 3 (b). This may be due to acid treatment, which likely introduces more surface defects, cracks, and pores, thereby enhancing potential adsorption and metal anchoring sites. Therefore, it can be concluded that nitric acid treatment significantly improved the surface morphology of PKSBC, resulting in a more fragmented and irregular texture compared to PKSBC. These results are consistent with those reported by Kim *et al.*, [11], who observed that nitric acid modification of activated carbon increased porosity and caused structural fragmentation through partial removal of carbon material and the introduction of functional groups. As shown in Figure 3 (c), the cerium loading at 1 wt.% on NA-PKSBC exhibits similar characteristics to NA-PKSBC, which has a rough and granular surface, but with small agglomerates likely representing cerium particles. Lou *et al.*, [12] reported similar findings when loading cerium oxides onto a support. Therefore, it can be concluded that cerium was successfully dispersed over the biochar surface, possibly anchored to



acid-functionalised sites. The pores appear partially blocked by fine nanoparticles, indicating successful metal incorporation but also a potential decrease in available surface area.

### 3.3. Textural Properties

The textural properties, including BET surface area, total pore volume, and average pore diameter of all synthesised catalysts, are summarised in Table 1. As shown in the table, the Ce/NA-PKSBC catalyst exhibited higher BET surface areas at 369.62 m<sup>2</sup>/g than the PKSBC (334.25 m<sup>2</sup>/g), except for NA-PKSBC, which showed a reduction at 272.36 m<sup>2</sup>/g. The decrease in surface area for NA-PKSBC compared to PKSBC is likely due to partial pore collapse and blockage caused by nitric acid treatment. This is supported by the FESEM image in Figure 3 (b), which shows irregular pore edges and potential obstruction. Additionally, the total pore volume of NA-PKSBC (0.1663 cm<sup>3</sup>/g) was lower than that of PKSBC (0.1876 cm<sup>3</sup>/g), further indicating that acid etching may have compromised the pore network. Similar findings were reported by Fu *et al.*, [13], who noted that acid treatment of biochar can lead to partial structural degradation, resulting in a reduction in surface area and pore volume.

**Table 1**

Textural properties of synthesized catalysts

Catalysts	<sup>a</sup> S <sub>BET</sub> (m <sup>2</sup> /g)	<sup>b</sup> V <sub>total</sub> (cm <sup>3</sup> /g)	<sup>c</sup> D (nm)
PKSBC	334.25	0.1876	2.25
NA-PKSBC	272.36	0.1663	2.44
Ce/NA-PKSBC	369.62	0.2166	2.34

<sup>a</sup>S<sub>BET</sub> (BET surface area) was obtained using Brunauer-Emmett-Teller.

<sup>b</sup>V<sub>total</sub> (total pore volume) was obtained from the adsorbed amount at P/P<sub>0</sub> = 0.99.

<sup>c</sup>D (average pore diameter) was obtained from the adsorption branches of the isotherm by BJH method.

Interestingly, upon cerium impregnation into NA-PKSBC, the BET surface area increased significantly to 369.62 m<sup>2</sup>/g, which is notably higher than that of both PKSBC and NA-PKSBC. This increase indicates successful metal incorporation, likely contributing to the development of additional pores or the formation of new mesoporous structures. The enhancement is further reflected in the total pore volume of Ce/NA-PKSBC, which increased to 0.2166 cm<sup>3</sup>/g, higher than PKSBC (0.1876 cm<sup>3</sup>/g) and NA-PKSBC (0.1663 cm<sup>3</sup>/g). These improvements in textural properties are supported by FESEM observations, as shown in Figure 3 (c), which reveal the presence of cerium agglomerates partially embedded in the rough surface. Together, these findings suggest that cerium loading not only modified the surface morphology but also enhanced the pore structure and surface accessibility of the catalyst.

### 3.4. Pyrolysis Product

The pyrolysis products were generally divided into two primary categories: condensable liquid products, which include both pyrolysis oil + wax, and non-condensable pyrolysis gases labelled as pyrolysis gas. Due to the difficulty in physically separating wax from oil at ambient conditions, they are reported together as a combined liquid yield. However, only the oil fraction was subjected to GC/MS analysis. Based on Figure 4, the pyrolysis product distribution for the benchmark catalysts, PKSBC and NA-PKSBC, shows relatively high yields of pyrolysis oil + wax at 60% and 68% respectively. The lower BET surface area and pore volume of NA-PKSBC compared to PKSBC (refer Table 1), suggest a more limited catalytic surface for vapour interaction and cracking. While nitric acid treatment increased surface roughness and introduced oxygen-containing functional groups, as shown in FESEM analysis, it also partially collapsed or blocked the pore network, potentially restricting vapour diffusion. Consequently, although NA-PKSBC yielded more total pyrolysis oil + wax than PKSBC, the product composition is likely more wax-dominant. This is because of structural limitations that hinder effective molecular breakdown or insufficient secondary cracking, as long-chain hydrocarbons remain unconverted.

Figure 4 also shows that the Ce/NA-PKSBC catalyst exhibited a markedly different product distribution compared to the benchmark catalysts, with a lower condensable fraction of 46% and a significantly higher gas yield of 54%. This shift indicates that cerium-based catalysts have vigorous cracking activity, capable of extensively breaking down long-chain hydrocarbons into smaller, non-condensable gaseous products [14]. While this demonstrates effective catalytic performance, it may be too aggressive for pyrolysis processes aimed at producing liquid fuels. Consequently, a large proportion of the pyrolysis vapour was converted into gas rather than remaining as liquid hydrocarbons. This limitation underscores the need to fine-tune the catalytic behaviour of cerium-based systems, a challenge addressed in subsequent catalysts through the addition of secondary metals to modulate activity and improve oil selectivity.

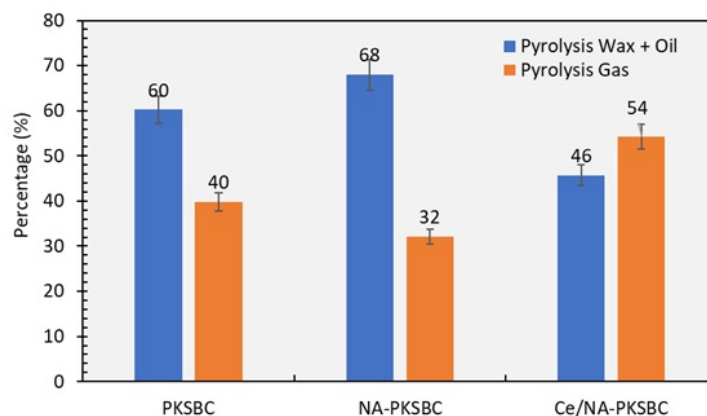


**Fig. 4.** Pyrolysis product yield of HDPE into pyrolysis oil + wax and pyrolysis gas

### 3.4. Organic Compositions in Pyrolysis Oil

Table 2 shows the composition of compounds identified in the pyrolysis oil derived from HDPE using different catalysts. The compounds are grouped into key functional categories, including hydrocarbons, ketones, phenols, alcohols, aldehydes, esters, carboxylic acids, ethers, nitrogen-

containing compounds, and others. These groups were identified based on GC/MS analysis of the condensable liquid fractions. Additionally, the data for non-catalytic pyrolysis are included for comparison to examine the effect of introducing catalysts, especially PKSBC and its modified derivatives, on the distribution and selectivity of pyrolysis products. It should be noted that several minor compounds, such as heterocyclic species, fluorinated compounds, phosphorus-containing compounds, siloxanes, and others, were detected in trace amounts during GC/MS analysis. These are most likely due to analytical artefacts, environmental contamination, or secondary reaction pathways, rather than direct products of HDPE pyrolysis. Since they contribute minimally to the total peak area and are of little relevance to the thermal degradation of polyolefins, they were not discussed in detail. However, nitrogen-containing compounds were kept and considered in the analysis, as they may stem from either HDPE additives or the nitric acid treatment used during catalyst preparation.

As shown in Table 2, the pyrolysis of HDPE yielded a hydrocarbon content of 63.38%, alongside a significant amount of carboxylic acids (19.45%) and nitrogen compounds (12.10%). The presence of these polar compounds is unexpected under an inert nitrogen atmosphere. However, it may originate from additives commonly found in commercial HDPE, such as stabilisers, plasticisers, and flame retardants, which contain heteroatoms like nitrogen and oxygen. Interestingly, the hydrocarbon content increased markedly to 97.58%, with a corresponding decrease in non-hydrocarbon compounds, when PKSBC act as the catalyst. This improvement may be attributed to the amorphous carbon structure of PKS-derived biochar, indicative of disordered carbon domains. The porous, irregular surface morphology observed in FESEM, combined with a relatively high BET surface area, probably facilitated effective vapour-surface interactions, promoting the cracking of long-chain waxes into hydrocarbons while simultaneously reducing oxygenate formation. Furthermore, the substantially decreased content of carboxylic acids (0.42%) and nitrogen-containing compounds (0.20%) in the PKSBC-catalysed oil demonstrates an improved selectivity for hydrocarbon formation, likely due to catalytic deoxygenation and adsorption of heteroatom species on the biochar surface.

**Table 2**  
Compounds in pyrolysis oil in all investigated samples

Compound s	Non- Catalytic	PKS BC	NA- PKSBC	Ce/NA- PKSBC
Hydrocarb ons	63.38	97.5 8	42.56	93.25
Ketones	-	0.34	0.29	-
Phenols	-	-	0.43	-
Alcohols	-	0.85	3.40	0.74
Aldehydes	0.19	-	1.90	3.43
Esters	2.73	0.42	10.81	-
Carboxylic acids	19.45	-	3.36	-
Ethers	-	-	0.40	0.23
N- Compounds	12.10	0.20	14.37	1.04
Other	2.15	0.64	22.40	1.35



Unlike PKSBC, the use of nitric acid-treated PKSBC (NA-PKSBC) led to a significant reduction in hydrocarbon selectivity, dropping from 97.58% to just 42.56%, as shown in Table 2. This sharp decline indicates that, although acid treatment usually aims to improve metal anchoring by adding oxygen-containing surface groups, it also causes adverse effects when applied without subsequent metal loading. The pyrolysis oil from NA-PKSBC-catalysed HDPE contained much higher amounts of carboxylic acids (3.36%) and nitrogen-containing compounds (14.37%), implying that the oxidative functionalisation during nitric acid treatment not only changed the surface chemistry but also involved secondary reactions. These nitrogenous compounds may come from reactions between pyrolysis intermediates and nitrogen-based functional groups introduced during acid treatment, or possibly from increased decomposition of HDPE additives in the presence of active acidic sites. Moreover, FESEM analysis showed a highly fragmented and irregular surface for NA-PKSBC, with increased surface roughness and visible microcracks (refer Figure 3), indicating a loss of thermal stability. This physical degradation, along with the lowest BET surface area and pore volume compared to PKSBC, may have decreased the effective contact area for hydrocarbon-forming reactions, instead encouraging side reactions and producing unwanted polar byproducts. These results highlight the need to balance surface modification with maintaining structural integrity and catalytic performance.

The pyrolysis oil derived from Ce/NA-PKSBC showed a hydrocarbon content of 93.25%, which, although relatively high, was lower than that obtained with PKSBC. This reduction aligns with the earlier product yield analysis, which showed that Ce/NA-PKSBC exhibited a significantly higher proportion of pyrolysis gas. The lower hydrocarbon content here may therefore be attributed to cerium's strong oxidative cracking ability, which promotes further degradation of condensable vapours into smaller, non-condensable gas molecules. Interestingly, Ce/NA-PKSBC produce higher detectable amounts of aldehydes (3.43%), a functional group not observed in the pyrolysis oils of the other samples. This suggests that the redox-active nature of cerium facilitates the oxidative cleavage or partial dehydrogenation of intermediate oxygenates, such as alcohols or carboxylic acids, into aldehydes. Shi *et al.*, [15] also found that  $\text{CeO}_2$  has a strong oxygen affinity as a promoter, activating oxygen-containing compounds and promoting oxygen removal. With the higher BET data showing a high surface area and FESEM revealing dispersed cerium particles anchored to the biochar surface, these features may contribute to enhanced interaction with oxygenated pyrolysis intermediates, leading to further transformation into aldehydes. While this highlights cerium's catalytic strength, it also reinforces the need to modulate its activity to minimise over-cracking and preserve liquid hydrocarbon selectivity. These findings underline the importance of metal synergy in adjusting the output of catalytic pyrolysis processes.

#### 4. Conclusions

In conclusion, this study demonstrated that cerium oxide-loaded nitric acid-treated palm kernel shell biochar (Ce/NA-PKSBC) exhibits distinct physicochemical properties and catalytic behaviour during the pyrolysis of high-density polyethylene (HDPE). The Ce/NA-PKSBC catalyst achieved the highest BET surface area ( $369.62 \text{ m}^2/\text{g}$ ) and total pore volume ( $0.2166 \text{ cm}^3/\text{g}$ ), indicating improved structural accessibility compared to untreated PKSBC. While Ce/NA-PKSBC achieved a high hydrocarbon yield of 93.25%, its strong cracking activity shifted product distribution towards non-condensable gases (54%), highlighting the need for activity modulation to optimise liquid fuel yields. The results suggest that integrating cerium oxide with nitric acid-functionalised biochar can enhance

catalytic efficiency and hydrocarbon selectivity, offering a sustainable alternative to conventional catalysts for plastic waste valorisation. Looking forward, future research should focus on fine-tuning metal loading and exploring bimetallic systems to balance cracking intensity and oil selectivity. Investigating the regeneration and long-term stability of Ce/NA-PKSBC under continuous pyrolysis conditions will be crucial for practical applications. Additionally, scaling up the process and conducting techno-economic analyses can help evaluate its commercial viability, while coupling with renewable hydrogen or co-feeding biomass could further improve product quality and align the process with circular economy and carbon-neutral goals.

### Acknowledgement

A special thanks to the Universiti Teknologi Malaysia (UTM) for the financial support to carry out this research project under the Potential Academic Staff (PAS), Cost Center No: Q.K130000.2743.03K72.

### References

- [1] Pandey, Dharen Kumar, Waleed M. Al-ahdal, Warren Rusere, Azwadi Ali, and Safwan Mohd Nor. "Impact of firm characteristics and country-level governance on global energy stocks during crises." *Research in International Business and Finance* 72 (2024): 102500. <https://doi.org/10.1016/j.ribaf.2024.102500>.
- [2] E. Chow, M. Xu, World is in its 'first truly global energy crisis' - IEA's Birol. Reuters. <https://www.reuters.com/markets/commodities/globaling-markets-further-tighten-next-year-ieas-birol-2022-10-25/>.
- [3] F. Zainal (2024). 39,000 tonnes of solid waste daily. The Star. <https://www.thestar.com.my/news/nation/2024/01/02/39000-tonnes-of-solid-waste-daily>
- [4] Rani, Aishwarya, Suraj Negi, Chihhao Fan, Su Shiung Lam, Hyunook Kim, and Shu-Yuan Pan. "Revitalizing plastic wastes employing bio-circular-green economy principles for carbon neutrality." *Journal of hazardous materials* 472 (2024): 134394. <https://doi.org/https://doi.org/10.1016/j.jhazmat.2024.134394>
- [5] Shahdan, Nadhilah Aqilah, Vekes Balasundram, Norazana Ibrahim, and Ruzinah Isha. "Catalytic co-pyrolysis of biomass and plastic wastes over metal-modified HZSM-5: A mini critical review." *Materials Today: Proceedings* 57 (2022): 1256-1261. <https://doi.org/https://doi.org/10.1016/j.apcata.2024.119581>
- [6] Daligaux, V., Romain Richard, M. Marin-Gallego, Valérie Ruaux, Ludovic Pinard, and M-H. Manero. "Deactivation by coking of industrial ZSM-5 catalysts used in LDPE pyrolysis and regeneration by ozonation process–Bench scale studies." *Applied Catalysis A: General* 671 (2024): 119581.
- [7] George, Jaise Mariya, Arun Antony, and Beena Mathew. "Metal oxide nanoparticles in electrochemical sensing and biosensing: a review." *Microchimica Acta* 185, no. 7 (2018): 358. <https://doi.org/10.1007/s00604-018-2894-3>
- [8] Dechapanya, Wipawee, and Attaso Khamwichit. "Biosorption of aqueous Pb (II) by H3PO4-activated biochar prepared from palm kernel shells (PKS)." *Heliyon* 9, no. 7 (2023). <https://doi.org/https://doi.org/10.1016/j.heliyon.2023.e17250>
- [9] Ryu, Hae Won, Do Heui Kim, Jungho Jae, Su Shiung Lam, Eun Duck Park, and Young-Kwon Park. "Recent advances in catalytic co-pyrolysis of biomass and plastic waste for the production

- of petroleum-like hydrocarbons." *Bioresource technology* 310 (2020): 123473.  
<https://doi.org/https://doi.org/10.1016/j.biortech.2020.123473>
- [10] Balasundram, Vekes, Norazana Ibrahim, Rafiziana Md Kasmani, Ruzinah Isha, Mohd Kamaruddin Abd Hamid, Hasrinah Hasbullah, and Roshafima Rasit Ali. "Catalytic upgrading of sugarcane bagasse pyrolysis vapours over rare earth metal (Ce) loaded HZSM-5: Effect of catalyst to biomass ratio on the organic compounds in pyrolysis oil." *Applied Energy* 220 (2018): 787-799. <https://doi.org/10.1016/j.apenergy.2018.03.141>
- [11] H.-K. Kim, S.-J. Kim, H.-R. Kim, J.-W. Park, Nitric acid modified powdered activated carbon for simultaneous adsorption of lead and phenol in aqueous solution. *Journal of Environmental Chemical Engineering*, 12(6) (2024), 114889.  
<https://doi.org/https://doi.org/10.1016/j.jece.2024.114889>
- [12] L. Lou, W. Li, H. Yao, H. Luo, G. Liu, J. Fang, Corn stover waste preparation cerium-modified biochar for phosphate removal from pig farm wastewater: Adsorption performance and mechanism. *Biochemical Engineering Journal*, 212 (2024), 109530.  
<https://doi.org/10.1016/j.bej.2024.109530>.
- [13] P. Fu, D. Zhang, B. Tang, X. Lin, H. Cai, Targeted production of aromatics from corn stover and high-density polyethylene composite pyrolysis over nitric acid modified biochar catalyst. *Journal of the Energy Institute*, 112 (2024), 101447.  
<https://doi.org/https://doi.org/10.1016/j.joei.2023.101447>.
- [14] Zhang, Bin, Ya'nan Li, Shuai Lu, Jonathan Richard Ishengoma, Song Wang, Jie Liu, Tao Tang, and Sanxi Li. "Inhibit effect of Pr, Ce, La or Yb doping on microwave-assisted pyrolysis of waste plastics for by-production oil over Co-Fe catalysts." *Journal of Analytical and Applied Pyrolysis* 179 (2024): 106485.  
<https://doi.org/10.1016/j.jaap.2024.106485>
- [15] F. Shi, J. Wang, H. Wang, C. Liu, Y. Lu, X. Lin, D. Hou, C. Wen, S. Yang, C. Luo, Z. Zheng, Y. Zheng, Increased high selectivity light aromatics and furans production by co-feeding methanol to catalytic pyrolysis of cellulose with Lanthanum–Cerium bimetallic modified MCM-41 catalysts. *Journal of the Energy Institute*, 108 (2023), 101206.  
<https://doi.org/https://doi.org/10.1016/j.joei.2023.101206>.